Nanoscale

Accepted Manuscript

This article can be cited before page numbers have been issued, to do this please use: Q. Al-Galiby, H. Sadeghi, L. Algharagholy, I. M. Grace and C. Lambert, *Nanoscale*, 2016, DOI: 10.1039/C5NR06966A.

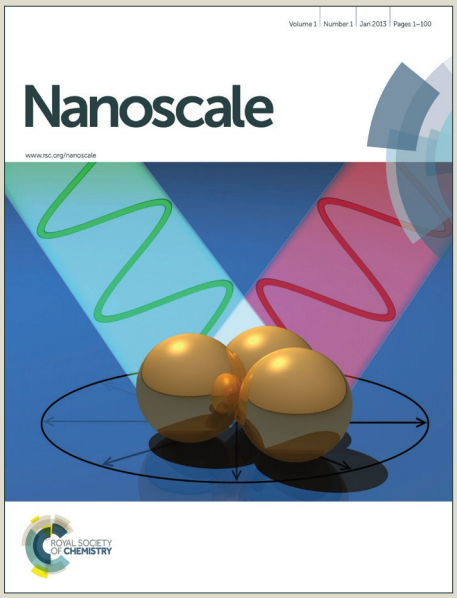

This is an *Accepted Manuscript*, which has been through the Royal Society of Chemistry peer review process and has been accepted for publication.

Accepted Manuscripts are published online shortly after acceptance, before technical editing, formatting and proof reading. Using this free service, authors can make their results available to the community, in citable form, before we publish the edited article. We will replace this *Accepted Manuscript* with the edited and formatted *Advance Article* as soon as it is available.

You can find more information about *Accepted Manuscripts* in the Information for Authors.

Please note that technical editing may introduce minor changes to the text and/or graphics, which may alter content. The journal's standard Terms & Conditions and the Ethical guidelines still apply. In no event shall the Royal Society of Chemistry be held responsible for any errors or omissions in this *Accepted Manuscript* or any consequences arising from the use of any information it contains.

ROYAL SOCIETY OF CHEMISTRY

www.rsc.org/nanoscale

View Article Online
DOI: 10.1039/C5NR06966A

Journal Name

ARTICLE

Tuning the thermoelectric properties of metallo-porphyrins

Qusiy H. Al-Galiby[†a,b], Hatef Sadeghi[†a], Laith A. Algharagholy[†a,c,d], Iain Grace[†a] and *Colin Lambert[†a]

Received 00th January 20xx,
Accepted 00th January 20xx

DOI: 10.1039/x0xx00000x
www.rsc.org/

We investigated the thermoelectric properties of metalloporphyrins connected by thiol anchor groups to gold electrodes. By varying the transition metal-centre over the family Mn, Co, Ni, Cu, Fe, and Zn we are able to tune the molecular energy levels relative to the Fermi energy of the electrodes. The resulting single-molecule room-temperature thermopowers range from almost zero for Co and Cu centres, to +80 μV/K and +230 μV/K for Ni and Zn respectively. In contrast, the thermopowers with Mn(II) or Fe(II) metal centres are negative and lie in the range -280 to -260 μV/K. Complexing these with a counter anion to form Fe(III) and Mn(III) changes both the sign and magnitide of their thermopowers to +218 and +95 respectively. The room-temperature power factors of Mn(II), Mn(III), Fe(III), Zn and Fe(II) porphyrins are predicted to be 5.9×10^{-5} W/m.K^2, 5.4×10^{-4} W/m.K^2, 9.5×10^{-4} W/m.K^2, 1.6×10^{-4} W/m.K^2 and 2.3×10^{-4} W/m.K^2 respectively, which makes these attractive materials for molecular-scale thermoelectric devices.

Introduction

The ability to generate a voltage from a temperature gradient has been known since the early 19th century[1]. This Seebeck effect is exploited to generate electricity from sources of waste heat such as automobile exhausts and industrial manufacturing processes and the inverse process (i.e. the Peltier effect) is used in cascade coolers for on-chip cooling of electronic devices[2-5]. Nowadays, a great deal of effort is aimed at increasing the efficiency of these effects and identifying the parameters that control the thermoelectric performance of materials and devices[6-12]. Although most common thermoelectric materials are inorganic, there is growing interest in the development of organic thermoelectric materials[6-10, 18-22], partly because many widely-deployed inorganic thermoelectric materials are toxic, expensive to process and have limited global supplies. Since the thermoelectric performance of inorganic materials can be enhanced by taking advantage of nanostructuring[13-19], there is particular interest in exploiting the room-temperature properties of single-molecules attached to nanogap electrodes, which can be regarded as the ultimate nanostructured devices. In what follows our aim is to explore the potential for thermoelectricity of single-molecule metallo-porphyrin junctions. Porphyrins are attractive as building blocks for molecular-scale devices, because they are conjugated, rigid, chemically stable and form metalloporphyrins by coordinating a variety of metallic ions[20-28].

From the point of view of optimising thermoelectric properties, junctions formed from these molecules are of interest, because by varying the metal atom residing in the core of the organic porphyrin framework, it should be possible to tune the molecular energy levels relative to the Fermi energy E_F of the electrodes. If energy levels can be caused to sit close to E_F, then this is expected to lead to transport resonances, which enhance the thermopower. In what follows, we shall demonstrate that this is indeed the case and that large positive and negative thermopowers are achievable.

Thermoelectric coefficients

To understand how transport resonances lead to high thermoelectric performance, we note that in the linear-response regime, the electric current I and heat current $\dot{\boldsymbol{Q}}$ passing through a device is related to the voltage difference ΔV and temperature difference ΔT by[29, 30]

$$\begin{pmatrix} I \\ \dot{Q} \end{pmatrix} = \frac{1}{h}\begin{pmatrix} e^2 L_0 & \frac{e}{T}L_1 \\ eL_1 & \frac{1}{T}L_2 \end{pmatrix}\begin{pmatrix} \Delta V \\ \Delta T \end{pmatrix} \qquad (1)$$

where T is the reference temperature. Since transport through single molecules is phase-coherent, even at room temperature, the coefficients L_n are given by $L_n = L_n^{\uparrow} + L_n^{\downarrow}$ $(n = 0, 1, 2)$, where

$$L_n^{\sigma} = \int_{-\infty}^{\infty} (E - E_F)^n \, T^{\sigma}(E)\left(-\frac{\partial f(E,T)}{\partial E}\right) dE \qquad (2)$$

In this expression, $T^{\sigma}(E)$ is the transmission coefficient for electrons of energy E, spin of $\sigma = [\uparrow, \downarrow]$ passing through the molecule from one electrode to the other[31] and $f(E,T)$ is Fermi distribution function defined as $f(E,T) = [e^{(E-E_F)/k_B T} + 1]^{-1}$ where k_B is Boltzmann's constant. Equation (1) can be rewritten in terms of the electrical conductance *(G)*, thermopower *(S)*, Peltier coefficient (∏), and the electronic contribution to the thermal conductance (κ_e):

$$\begin{pmatrix} \Delta V \\ \dot{Q} \end{pmatrix} = \begin{pmatrix} 1/G & S \\ \prod & \kappa_e \end{pmatrix}\begin{pmatrix} I \\ \Delta T \end{pmatrix} \qquad (3)$$

where

[a] Quantum Technology Centre, Lancaster University, Lancaster LA1 4YB, UK.
[b] Physics Department ,Al-Qadisiyah University, Diwaniyah, 58002, IRAQ
[c] College of Basic Education, Sumer University, Al-Refayee, Thi-Qar 64001, IRAQ
[d] College of Computer Science and Mathematics, Al-Qadisiyah University, Al-Qadisiyah ,Diwaniyah, 58002, IRAQ.
† Authors contributed equally.
*Corresponding author: c.lambert@lancaster.ac.uk, qusiyalgaliby@gmail.com
Electronic Supplementary Information (ESI) available: [details of any supplementary information available should be included here]. See DOI: 10.1039/x0xx00000x

View Article Online
DOI: 10.1039/C5NR06966A

$$G = \frac{e^2}{h} L_0 \quad (4)$$

$$S = -\Delta V/\Delta T = \frac{1}{eT}\frac{L_1}{L_0} \quad (5)$$

$$\Pi = \frac{1}{e}\frac{L_1}{L_0} \quad (6)$$

$$\kappa_e = \frac{1}{hT}\left(L_2 - \frac{(L_1)^2}{L_0}\right) \quad (7)$$

From the above expressions, the electronic thermoelectric figure $ZT_e = S^2GT/\kappa_e$ is given by

$$ZT_e = \frac{(L_1)^2}{L_0 L_2 - (L_1)^2} \quad (8)$$

For E close to E_F, if $T(E)$ varies only slowly with E on the scale of k_BT then these formula take the form[32]:

$$G(T) \approx \left(\frac{2e^2}{h}\right) T(E_F), \quad (9)$$

$$S(T) \approx -\alpha e T \left(\frac{d\, lnT(E)}{dE}\right)_{E=E_F}, \quad (10)$$

$$\kappa_e \approx L_0^{\sigma} TG, \quad (11)$$

where $\alpha = \left(\frac{k_B}{e}\right)^2 \frac{\pi^2}{3}$ is the Lorentz number. Equation (10) demonstrates that S is enhanced by increasing the slope of ln $T(E)$ near $E=E_F$ and hence it is of interest to explore whether or not the ability to vary the metal centre in metallo-porphyrins can be used to move resonances close to E_F.

Methods

As shown in Figure 1, the porphyrin monomer of interest consists of four pyrrole cores (the inner ring π-system) with side groups comprising a phenyl ring connected via two oxygen atoms to electrically-inert alkyl groups (-C8H17). The core of porphyrin is connected via thiol anchor groups to gold electrodes. Our aim

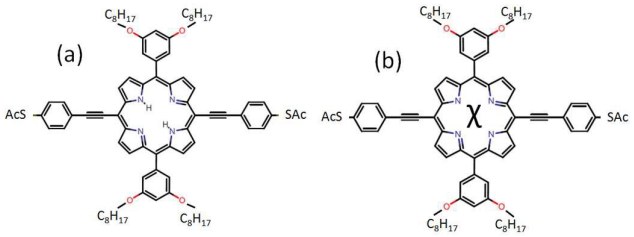

Figure 1: Porphyrin-based molecular structures (a) without metallic atom, (b) with different metallic atoms χ = Co, Cu, Fe, Mn, Ni, and Zn

in this paper is to investigate the effect on thermoelectric performance of varying the metal atom χ over the series of χ = Co, Cu, Fe, Mn, Ni, and Zn.

To calculate the electrical properties of each metallo-porphyrin, we used the spin density functional theory (DFT) code SIESTA[33] which employs Troullier-Martins pseudopotentials to represent the potentials of the atomic cores[34], and a local atomic-orbital basis set. A double-zeta polarized basis set was used for all atoms and the generalized gradient approximation (GGA-PBE) for the exchange and correlation functionals[35, 36]. The Hamiltonian and overlap matrices are calculated on a real-space grid defined by a plane-wave cut-off of 150 Ry. Each molecule was relaxed to the optimum geometry until the forces on the atoms are smaller than 0.02 eV/Å and in case of the isolated molecules, a sufficiently-large unit cell was used to avoid inter-cell interactions. All porphyrin molecules with metallic atoms χ were found to be slightly twisted after relaxation.

After obtaining the relaxed geometry of each isolated molecule, the molecules were placed between two gold electrodes, as shown in Figure 2. For structures such as those shown in Figure 2, the central region of the junction is composed of a single molecule attached to two gold (111) leads. The equilibrium distance between the sulfur atom of each anchor group and the centre of the apex atom of each gold pyramid was initially 2.5 Å. After geometry optimization the distance changed slightly from the initial value to a final value of 2.63 Å.

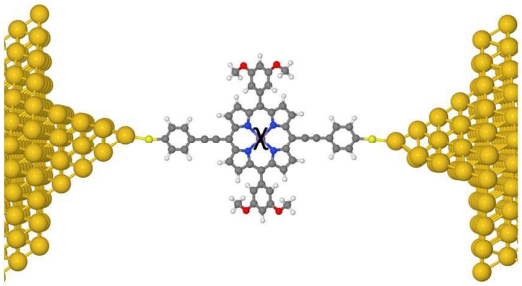

Figure 2. An example of an optimized junction configuration. To reduce the computational cost, we replace the electrically-inert alkyl group (-C8H17) with a methyl group (-CH3).

The *d*-orbitals of metallic atoms could be partially filled, so for each molecular junction, we carried out a spin-polarized calculation to obtain the electron and spin transport properties, using the Gollum quantum transport code[37] to compute the spin-dependent transmission coefficients $T^{\sigma}(E)$ for electrons of energy E passing from the left gold electrode to the right electrode. Gollum is a next-generation code, born out of the SMEAGOL code[38] and uses the mean-field Hamiltonian and overlap matrices obtained from density functional theory to compute transport properties of a wide variety of nanostructures. After computing $T^{\sigma}(E)$, we evaluated the zero-bias thermoelectric coefficients over a wide range of Fermi energies and temperatures by using equations (1-8).

Results and Discussion

For each metallo-porphyrin P-χ in Figure 1b, the charge transfer between the metal atom and the porphyrin framework was calculated (as shown in Table S1 of SI). As expected, the calculations show that all metal atoms donate electrons to the porphyrin host. As examples, Figure 3 shows the frontier orbitals, spin-dependent and total transmission coefficients of the bare porphyrin (left) and Fe-porphyrin (right) relative to the DFT-predicted Fermi energy E_F^{DFT}. Results for other molecules are shown in figures (S1-S7) of the SI.

Figure 3(a) shows that for the bare porphyrin, the transmission T(E) at the DFT-given Fermi level (E_F^{DFT}, indicated by the vertical black line) is closest to the HOMO resonance and the slope of the curve is negative. On the other hand for the Fe porphyrin, figure 3b shows that the Fermi level is nearest to the LUMO resonance and the slope is positive in both Figures 3b. Hence from equation (10), one expects the thermopower of the former (latter) to be positive (negative).

View Article Online
DOI: 10.1039/C5NR06966A

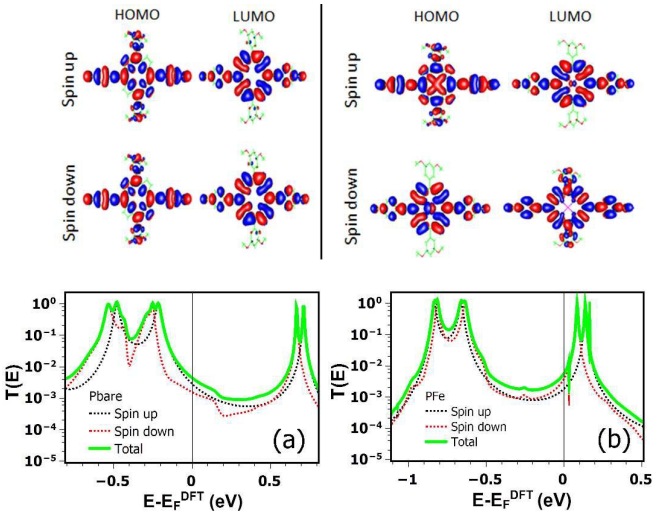

Figure 3. Top panels: Iso-surfaces of frontier molecular orbitals of the bare porphyrin (Porphyrin -bare) and the iron-porphyrin (Porphyrin-Fe(II) obtained using spin- polarized DFT. Red corresponds to positive and blue to negative regions of the wave functions. Lower panels: The spin-dependent and total transmission coefficients as a function of energy for bare porphyrin (left) and porphyrin-Fe (right).

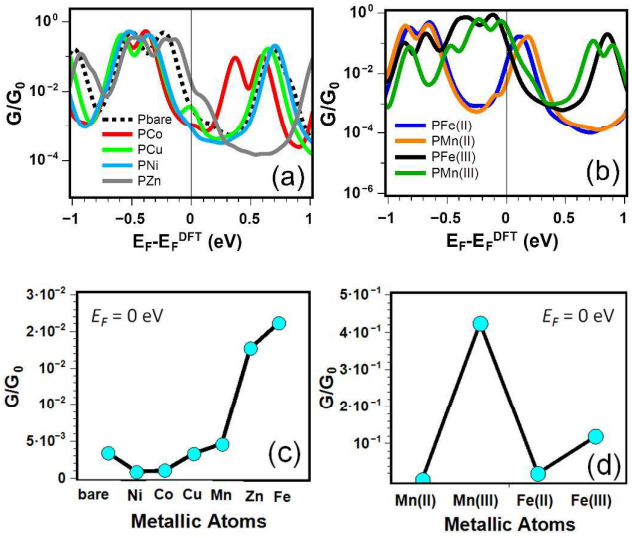

Figure 4. (colour online) DFT spin-dependent room-temperature electrical conductance (in units of $G_0 = 2e^2/h$ = 77 μSiemens) over a range of Fermi energies for (a) the P-bare and P-Co, Cu, Ni and Zn and (b) the P-bare and P-Fe(II), P-Mn(II), PFe(III) and PMn(III). (c) Room-temperature values of G for P-bare, P-Co, P-Cu, P-Ni, P-Zn, P-Fe(II) and P-Mn(II) are 3.43 ×10^{-3}, 1.05 ×10^{-3}, 3.48 ×10^{-3}, 8.7 ×10^{-4}, 1.7 ×10^{-2} and 2.1 ×10^{-2} respectively. (d) Room-temperature values of G for the porphyrins Mn(II), Mn(III), Fe(II) and Fe(III). The lines in (c) and (d) are guides to the eye.

Figure 4 shows the total room temperature electrical conductance for each P-χ. Figure 4(a) shows that the bare (dotted line) and Co, Cu, Zn and Ni porphyrins (solid lines), exhibit HOMO-dominated conductance at the DFT Fermi energy,

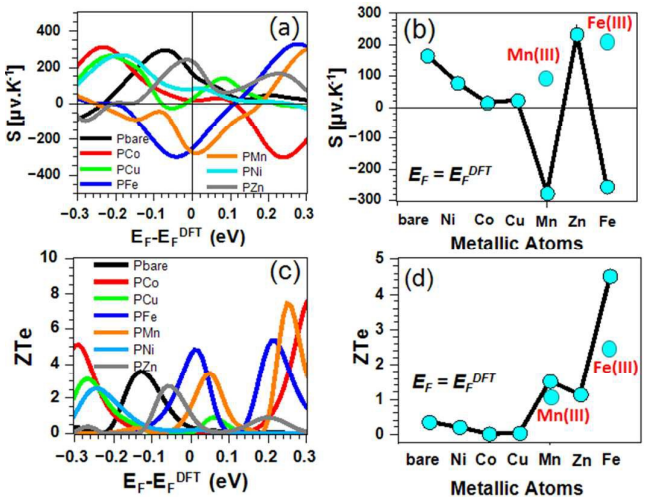

Figure 5. The room-temperature thermopower S and figure of merit ZT_e. 4(a) and (c) show plots of S and ZT_e over a range of Fermi energies E_F relative to the DFT-predicted Fermi energy E_F^{DFT}. The right column shows room-temperature values obtained using $E_F = E_F^{DFT}$. of S and ZT_e for each metallo-porphyrin.

whereas Figure 4b shows that for the Mn(II) and Fe(II) porphyrins, we obtain LUMO-dominated conductance. Figure 4(c) shows the room-temperature conductance at the DFT Fermi energy and shows that the pattern of increasing conductance is Ni < Co < Cu < Bare < Mn(II) < Zn < Fe(II). The conductance of porphyrin-Cu (3.49×10^{-3} G_0) is slightly higher than of porphyrin-bare, (3.43×10^{-3} G_0). This order is in agreement with previous measurements on similar molecules[25]. We are not aware of conductance measurements of the Mn, Zn and Fe porphyrins.

In the case of Mn and Fe, metalloporphyrins exist more commonly as P-M(III) in the presence of a counter anion. Since it is straightforward to oxidise/reduce between Fe(II)/(III) and Mn(II)/(III), we have also computed all thermoelectric properties for Fe(III) and Mn(III) complexed with a Cl^- counter ion (See SI Figures S9–S15). The resulting room-temperature conductances are shown in Figure 4b reveals that in the presence of the counter anion, transport becomes LUMO dominated. Figure 4d compares the room-temperature conductances of Fe(II)/(III) and Mn(II)/(III) and shows that the presence of a counter anion increases the electric conductance.

Figures 5b and 5d show results for the Seebeck coefficient (thermopower) S and electronic contribution to the figure of merit ZT_e at room temperature. It is well-known that DFT can give inaccurate value for the Fermi energy and therefore Figures 5a and 5c show corresponding results for a range of Fermi energies E_F relative to the DFT-predicted Fermi energy E_F^{DFT}, whereas Figures 5b and 5d show room-temperature values of S and ZT_e for each metallo-porphyrin, evaluated at the DFT Fermi energy. Figure 5b demonstrates that both the magnitude and sign of thermopower S are sensitive to the metal atoms at the centre of the porphyrin monomer, which determine the location of transport resonances relative to the Fermi energy. Furthermore, in the case of Fe and Mn, Figure 5b reveals that the sign of the thermopower can be switched from negative to positive upon complexation with Cl^-, due to their switching from HOMO to LUMO dominated transport.

At the DFT-predicted Fermi energy, the highest values of the thermopower are obtained in the presence of Mn, Fe and Zn, for which S takes values -280, -260 and +230 μV/K respectively, all of which have a greater magnitude than the

View Article Online
DOI: 10.1039/C5NR06966A

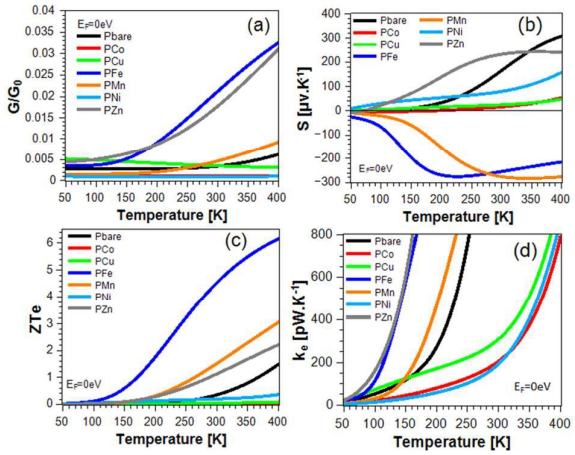

Figure 6: (a, b, c and d) represent the electrical conductance, Seebeck coefficients *S* (thermopower), electronic contribution to the figure of merit ZT_e and electronic contribution to the thermal conductance k_e over a range of temperatures, evaluated at $E_F = E_F^{DFT}$.

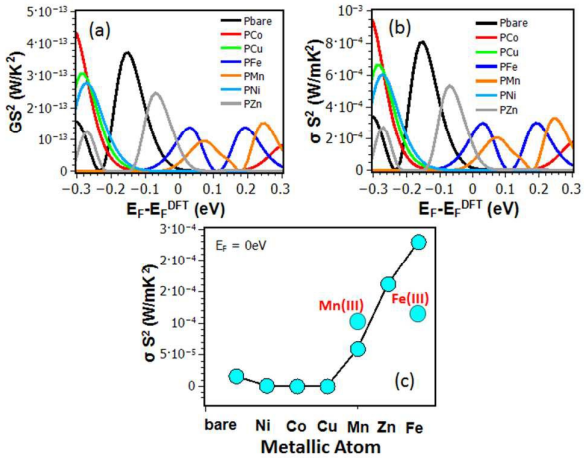

Figure 7: The upper figure (a) shows room-temperature values of the product GS^2, while figure (b) shows the power factor $P = S^2GL/A$ evaluated at $E_F = E_F^{DFT}$. The lower figure (c) shows room-temperature values of power factor $P = S^2GL/A$ for each metallo-porphyrin.

thermopower of the bare porphyrin (165 μV/K). The lowest values of all are obtained for Co, closely followed by Cu. For Fe(III)-P we obtain S= +218 μV/K at room temperature and for Mn(III)-P we find S= +95 μV/K. Corresponding results for the electronic contribution to the figure of merit ZT_e are shown in Figure 5d. The highest values of ZT_e are obtained in the presence of Zn, Mn and Fe, reflecting the high values of their thermopowers and conductances.

Figure 6 shows the electrical conductance G, Seebeck coefficients *S* (thermopower), electronic contribution to the figure of merit ZT_e and electronic contribution to the thermal conductance k_e as a function of temperature, obtained using the DFT-predicted Fermi energy E_F^{DFT}. These results show that the magnitudes of all quantities increase with increasing temperature.

A crucial quantity determining the efficiency of a thermoelectric material or device is the dimensionless figure of merit $ZT = S^2GT/\kappa$, whose denominator κ is the total thermal conductance due to both phonons and electrons. This differs from the electronic figure of merit $ZT_e = S^2GT/\kappa_e$ whose denominator contains only the thermal conductance due to electrons. For a bulk material, *ZT* is often written in the form $= (P/\kappa)T$, where κ is the total thermal conductivity and *P* is the power factor defined by as $P = S^2\sigma$, where σ is the electrical conductivity. In practice for a single molecule, *ZT* is difficult to measure experimentally, because the thermal conductance κ of a single molecule is not directly accessible. However the numerator of ZT (i.e. the power factor P) is accessible. The notion of conductivity is not applicable to transport through single molecules, but to compare with literature values for bulk materials, we define $\sigma = \mathrm{GL/A}$, where L and A are equal to the length and the cross-sectional area of the molecule respectively. In what follows, the values $\mathrm{L} = 4.0\ \mathrm{nm}$ and $\mathrm{A} = 1.8\ \mathrm{nm}^2$ are used. From the results of Figure 5, the quantity GS^2 and power factors $P = S^2GL/A$ for each of the studied molecules are shown in Figure 7.

These results show that Mn, Mn(III), Fe(III), Zn and Fe porphyrins have the highest power factors of 5.9×10^{-5} W/m.K^2, 5.4×10^{-4} W/m.K^2, 9.5×10^{-4} W/m.K^2, 1.6×10^{-4} W/m.K^2 and 2.3×10^{-4} W/m.K^2 respectively.

Conclusion

We have used spin-dependent density functional theory to study the thermoelectric properties of metallo-porphyrin monomers with central metal atoms chosen from the series Co, Cu, Fe, Mn, Ni, and Zn. We found that the energies of transport resonances can be tuned through the choice of central metal atom, leading to large negative thermopowers in the range -280 to -260 μV/K for Mn(II)- and Fe(II)-porphyrins and a large positive thermopower of +230 μV/K in the case of Zn-porphyrin. These Seebeck coefficients are almost independent of temperature at room temperature and are significantly larger than recently-measured values of *S* at room temperature. For example, measured values include 8.7, 12.9 and 14.2 *μV/K* for 1,4-benzenedithiol (BDT), 4,4′-dibenzenedithiol, and 4,4′′-tribenzenedithiol respectively[39], -1.3 to 8.3 *μV/K* for the benzene-based series of benzene-dithiol (BDT), 2,5-dimethyl-1,4-benzenedithiol (BDT2Me), 2,3,5,6-tetrachloro-1,4-benzenedithiol (BDT4Cl), 2,3,5,6-tetraflouro-1,4-benzenedithiol (BDT4F) and BDCN[40, 41], 7.7 to 15.9 *μV/K* for the series BDT, DBDT, TBDT and DMTBDT[42], -12.3 to 13.0 *μV/K* for a series of amine-Au and pyridine-Au linked molecules[43] and -8.9 to -33.1 *μV/K* for fullerene-based single-molecule junctions[9, 40, 44]. Furthermore Zn-porphyrins have a large electronic figures of merit. At room temperature, we obtain power factors of 5.9×10^{-5} W/m.K^2 for Mn-porphyrin, 5.4×10^{-4} W/m.K^2 For Mn(III)-porphyrin, 9.5×10^{-4} W/m.K^2 for Fe(III)-porphyrin, 1.6×10^{-4} W/m.K^2 for Zn-porphyrin and 2.3×10^{-4} W/m.K^2 for Fe(II)-porphyrin. These compare favourably with power factors of other organic materials, whose reported values range from 0.016 μW/m.K^2 and 0.045 μW/m.K^2 for Polyaniline and Polypyrole respectively [45], to 12 μW/m.K^2 for PEDOT:PSS [46] and (12 μW/m.K^2 for C_{60}/Cs_2Co_3 Dph-BDT [47].

This ability to tune the thermoelectric properties of single molecules, combined with the fact that the Seebeck coefficient is an intrinsic property, which does not scale with the number of molecules conducting in parallel, suggests that self-assembled monolayers or few-layers of metallo-porphyrins have potential for high-performance conversion of heat into electricity and efficient Peltier cooling**.** The technical step of translating single-molecule properties into thin films is a significant challenge and a major programme of

View Article Online
DOI: 10.1039/C5NR06966A

fundamental research will be needed to fully address this issue. Nevertheless our recent theoretical study of the thermal conductance of single alkane and alkyne molecules compares favourably with experiments on thin films of such molecules[48] and gives us confidence single-molecule thermal properties do survive in molecular films. Furthermore many of the techinical barriers to be overcome are already clear. For example, to take advantage of the quantum effects described in this paper, the film thickness should be less than the electronic phase-breaking length, which at room temperature is of order 3nm[49-51]. If molecules are first deposited onto a bottom electrode, then the top electrode should be added without destroying the integrity of the molecular film. One solution to the "top-contact problem" would be to use a two-dimensional electrode material such as graphene as the top electrode. Success would depend on alignment or misalignment of the two contacts and the presence of step edges and other defects in the transferred two-dimensional material. In the case of hexagonal materials such as graphene, such defects would include non-hexagonal rings[52], which would alter the binding energy and electronic coupling to molecular anchor groups. It is well established that both molecules and electrodes should be treated in an holistic manner when designing single-molecule junctions[53] and the same will be true of thin films. For the purpose of increasing *ZT* and reducing the thermal conductance, one strategy will involve choosing electrode materials which maximise phonon scattering at the molecule-electrode interface and taking advantage of phonon filtering by the electrodes, as a described in[48]. In addition, intermolecular interactions may utilised to optimise thin-film properties beyond those accessible to single molecules.

Acknowledgment

This work is supported by the UK EPSRC, EP/K001507/1, EP/J014753/1, EP/H035818/1, and from the EU ITN MOLESCO 606728 and the Higher Education Ministry, Al Qadisiyah University, IRAQ.

References

1 T.J. Seebeck, Annalen der Physik, 82 (1826) 253-286.
2 X. Chen, L. Chen, J. Guo, J. Chen, international journal of hydrogen energy, 36 (2011) 6099-6104.
3 S. Kumar, S.D. Heister, X. Xu, J.R. Salvador, G.P. Meisner, Journal of electronic materials, 42 (2013) 665-674.
4 B.I. Ismail, W.H. Ahmed, Recent Patents on Electrical & Electronic Engineering (Formerly Recent Patents on Electrical Engineering), 2 (2009) 27 39.
5 D. Voneshen, K. Refson, E. Borissenko, M. Krisch, A. Bosak, A. Piovano, E. Cemal, M. Enderle, M. Gutmann, M. Hoesch, Nature materials, 12 (2013) 1028-1032.
6 M. Bürkle, L.A. Zotti, J.K. Viljas, D. Vonlanthen, A. Mishchenko, T. Wandlowski, M. Mayor, G. Schön, F. Pauly, Physical Review B, 86 (2012) 115304.
7 P. Chaikin, J. Kwak, Review of Scientific Instruments, 46 (1975) 218-220.
[8] S.-H. Ke, W. Yang, S. Curtarolo, H.U. Baranger, Nano letters, 9 (2009) 1011-1014.
9 C. Evangeli, K. Gillemot, E. Leary, M.T. González, G. Rubio-Bollinger, C.J. Lambert, N. Agrait, Nano letters, 13 (2013) 2141-2145.
10 A.A. Balandin, Nature Materials, 10 (2011) 569-581.
11 H. Sadeghi, S. Sangtarash, C.J. Lambert, Scientific reports, 5 (2015) 9514.
12 H. Sadeghi, S. Sangtarash, C.J. Lambert, Beilstein Journal of Nanotechnology, 6 (2015) 1176-1182.
13 R. Venkatasubramanian, E. Siivola, T. Colpitts, B. O'quinn, Nature, 413 (2001) 597-602.
14 T. Harman, P. Taylor, M. Walsh, B. LaForge, Science, 297 (2002) 2229-2232.
15 B. Poudel, Q. Hao, Y. Ma, Y. Lan, A. Minnich, B. Yu, X. Yan, D. Wang, A. Muto, D. Vashaee, Science, 320 (2008) 634-638.
16 X. Liu, D. Wang, J. Shi, APS Meeting Abstracts2011, pp. 30013.
17 K. Yanagi, S. Kanda, Y. Oshima, Y. Kitamura, H. Kawai, T. Yamamoto, T. Takenobu, Y. Nakai, Y. Maniwa, Nano letters, 14 (2014) 6437-6442.
18 A. Kambili, G. Fagas, V.I. Fal'ko, C. Lambert, Physical Review B, 60 (1999) 15593.
19 G. Fagas, A. Kozorezov, C. Lambert, J. Wigmore, A. Peacock, A. Poelaert, R. Den Hartog, Physical Review B, 60 (1999) 6459.
20 G. Dorough, J. Miller, F.M. Huennekens, Journal of the American Chemical Society, 73 (1951) 4315-4320.
21 G. Sedghi, V.M. García-Suárez, L.J. Esdaile, H.L. Anderson, C.J. Lambert, S. Martín, D. Bethell, S.J. Higgins, M. Elliott, N. Bennett, Nature nanotechnology, 6 (2011) 517-523.
22 D. Gust, J.D. Roberts, Journal of the American Chemical Society, 99 (1977) 3637-3640.
23 Z. Li, M. Smeu, M.A. Ratner, E. Borguet, The Journal of Physical Chemistry C, 117 (2013) 14890-14898.
24 Z. Li, E. Borguet, Journal of the American Chemical Society, 134 (2011) 63-66.
25 Z.-F. Liu, S. Wei, H. Yoon, O. Adak, I. Ponce, Y. Jiang, W.-D. Jang, L.M. Campos, L. Venkataraman, J.B. Neaton, Nano letters, 14 (2014) 5365-5370.
26 Y. Li, J. Yao, S. Zhong, Z. Zou, Current Applied Physics, 11 (2011) 1349-1353.
27 R. Ferradás, V.M. García-Suárez, J. Ferrer, arXiv preprint arXiv:1208.3157, (2012).
28 I. Beletskaya, V.S. Tyurin, A.Y. Tsivadze, R. Guilard, C. Stern, Chemical reviews, 109 (2009) 1659-1713.
29 V.V. Maslyuk, S. Achilles, I. Mertig, Solid State Communications, 150 (2010) 505-509.
30 V.M. García-Suárez, R. Ferradás, J. Ferrer, Physical Review B, 88 (2013) 235417.
31 N. Claughton, C. Lambert, Physical Review B, 53 (1996) 6605.
32 V.M. García-Suárez, C.J. Lambert, D.Z. Manrique, T. Wandlowski, Nanotechnology, 25 (2014) 205402.
33 J.M. Soler, E. Artacho, J.D. Gale, A. García, J. Junquera, P. Ordejón, D. Sánchez-Portal, Journal of Physics: Condensed Matter, 14 (2002) 2745.
34 N. Troullier, J.L. Martins, Physical Review B, 43 (1991) 1993.
35 J.P. Perdew, K. Burke, M. Ernzerhof, Physical review letters, 77 (1996) 3865.
36 B. Hammer, L.B. Hansen, J.K. Nørskov, Physical Review B, 59 (1999) 7413.
37 J. Ferrer, C.J. Lambert, V.M. García-Suárez, D.Z. Manrique, D. Visontai, L. Oroszlany, R. Rodríguez-Ferradás, I. Grace, S. Bailey, K. Gillemot, New Journal of Physics, 16 (2014) 093029.
38 A.R. Rocha, V.M. Garcia-Suarez, S.W. Bailey, C.J. Lambert, J. Ferrer, S. Sanvito, Nature materials, 4 (2005) 335-339.
39 P. Reddy, S.-Y. Jang, R.A. Segalman, A. Majumdar, Science, 315 (2007) 1568-1571.
40 J.A. Malen, S.K. Yee, A. Majumdar, R.A. Segalman, Chemical Physics Letters, 491 (2010) 109-122.
41 K. Baheti, J.A. Malen, P. Doak, P. Reddy, S.-Y. Jang, T.D. Tilley, A. Majumdar, R.A. Segalman, Nano letters, 8 (2008) 715-719.
42 J.A. Malen, P. Doak, K. Baheti, T.D. Tilley, A. Majumdar, R.A. Segalman, Nano letters, 9 (2009) 3406-3412.
43 J.R. Widawsky, P. Darancet, J.B. Neaton, L. Venkataraman, Nano letters, 12 (2011) 354-358.
44 S.K. Yee, J.A. Malen, A. Majumdar, R.A. Segalman, Nano letters, 11 (2011) 4089-4094.
45 A. Shakouri and S. Li, S. In Thermoelectrics, 1999. Eighteenth International Conference on (pp. 402-406). IEEE.
46 H. Shi, C. Liu, J. Xu, H. Song, Q. Jiang, B. Lu, and F. Jiang, Int. J. Electrochem. Sci 9 (2014): 7629-43.
47 M. Sumino, K. Harada, M. Ikeda, S. Tanaka, K. Miyazaki, C. & Adachi, Applied Physics Letters (2011) 99.9: 093308.

View Article Online
DOI: 10.1039/C5NR06966A

48 H. Sadeghi, S. Sangtarash and C.J. Lambert, *Nano Lett.*, **2015**, *15* (11), pp 7467–7472

49 H. Sadeghi, J.A. Mol, C.S. Lau, G.A.D. Briggs, J. Warner, C.J. Lambert, *Proc. Natl. Acad. Sci.* (2015), *112*, 2658.

50 G. Sedghi, V.M. García-Suárez, L.J. Esdaile, H.L. Anderson, C.J. Lambert, S. Martín, D. Bethell, S.J. Higgins, M. Elliott, N. Bennett, *Nat. Nanotechnol.* (2011), *6*, 517.

51 X. Zhao, C. Huang, M. Gulcur, A.S. Batsanov, M. Baghernejad, W. Hong, M.R. Bryce, T. Wandlowski, *Chem. Mat.* (2013), *25*, 4340.

52 C.J. Lambert and D.L. Weaire, Metallography (1981) 14 (4), 307

53 W. Haiss, C. Wang, R. Jitchati, I. Grace, S. Martín, A.S. Batsanov, S.J. Higgins, M.R. Bryce, C.J. Lambert, P.S. Jensen, R.J. Nichols, J. Phy.s: Condensed Matter 20 (37), 374119